Resonant photoemission study of ScF_3 at the Sc $2p$ and F $1s$ absorption edges: Observation of the satellite structure due to the strong hybridization effect

M. Umeda, Y. Tezuka, and S. Shin*
Synchrotron Radiation Laboratory, Institute for Solid State Physics, University of Tokyo, 3-2-1 Midoricho, Tanashi-shi, Tokyo 188, Japan

A. Yagishita
Photon Factory, National Laboratory for High Energy Physics (KEK), Tsukuba-shi, Ibaraki 305, Japan
(Received 2 June 1995)

The electronic structure of ScF_3 has been investigated by resonant photoemission at the Sc $2p$ and F $1s$ absorption edges. At off-resonant photoemission, a charge-transfer-type satellite is found with an energy separation of about 13 eV below main peaks in valence-band and various core-energy regions. Another satellite is found with an energy separation of about 9–10 eV and its intensity is strongly enhanced at the excitation energy of Sc $2p$ and F $1s$ thresholds. It is found to be the charge-transfer satellite that is caused by the strong hybridization effect between Sc $3d$ and F $2p$ states in the valence band.

I. INTRODUCTION

Scandium, titanium, and vanadium metals are located at the beginning of the series of the $3d$ transition metals and are called early transition metal. In a simple ionic model, their compounds have no $3d$ electrons nominally in the ground state and the valence band (VB) are filled up with the ligand electrons. Recently, it has been suggested that the hybridization effect between the $3d$ and ligand orbitals is very important in the early transition-metal compounds.[1–6] In the previous paper,[7] we reported on an investigation of the electronic structure of ScF_3 by the resonant photoemission at the Sc $3p$ absorption edge. The VB satellites were observed in the early transition-metal compounds, such as ScF_3, TiO_2, and V_2O_5. The energy separation between the satellite and the main VB peak is about 13 eV for Sc compounds. It decreases from Sc to V compounds according to the increase of the atomic number. The intensity of the satellite becomes weak and broad with the increase of the atomic number. Because of the resonant enhancement of the satellite near the Sc $3p$ absorption edge, the $3d$ character is evident for the satellite structure. That is, it is assigned to be a kind of a charge-transfer (CT) satellite. By the many-body configuration-interaction (CI) representation,[8–13] the CT satellite is mainly ascribed to the $3d^1\underline{L}^2$ state in the final state, while the main line is mainly ascribable to the $3d^0\underline{L}$ state. Here, the $\underline{L}$ represents the hole state in the VB and $\underline{L}^2$ represents the two-hole state in the VB.

There is a problem that the energy separation of the satellite is too large compared to the magnitude of the charge-transfer energy Δ, because it is about 7–8 eV. Recently Okada and Kotani[2] calculated the CT satellite in the Ti $2p$ core-energy region of Ti compounds. The large energy separation of the satellite structure is well reproduced by the calculation, where the large energy separation is due to the large hybridization effect V rather than the CT energy. It is roughly determined to be $\sqrt{\Delta^2+4V_{\rm eff}^2}\approx 2V_{\rm eff}$; where $V_{\rm eff}$ is $\sqrt{6V(t_{2g})^2+4V(e_g)^2}$ and $V(t_{2g})$ and $V(e_g)$ are the hybridization energies for t_{2g} and e_g states.

The study of scandium compounds has been very limited.[14–17] de Boer, Haas, and Sawatzky[14] found the strong satellite structure in the Sc $2p$ photoemission of various Sc compounds. The energy separation from the main peak is found to be about 13 eV. The satellite structure has a prominent chemical tendency. That is, the energy separation and the intensity decrease from ScF_3 to ScI_3 compounds. Thus, the large energy separation was elucidated by the excitonic (polaron) effect that causes the transition from occupied p to empty s states within the ligand ion, due to the created Sc $2p$ core hole. By this assignment, the satellite component is not of Sc $3d$ character, but of ligand-p character.

In this study, the measurements of Sc $2p$ and F $1s$ resonant photoemission of ScF_3, as well as Sc $3p$ resonant photoemission, are carried out in order to make clear the origin of the satellite. Since the scandium metal is located at the beginning of the series of the $3d$ transition metals, their compounds are the most ionic of the transition-metal compounds. We believe that the role of hybridization effect between the $3d$ and ligand orbitals becomes clear, because the effect of $3d$-electron interaction is the weakest of the transition-metal compounds, because of few $3d$-electron numbers and a weak electron correlation energy. In the other transition metal compounds, the $3d$-electron interaction is so strong that the spectra are very complicated in general and are often smeared out.[18–20] Furthermore, it is known that the resonant photoemission is a powerful method to observe the $3d$ components in the spectra.

II. EXPERIMENT

The thin film of ScF_3 was evaporated on the gold substrate from the tungsten basket. In order to prevent the charging up effect of the samples, the thickness of the sample is about 50–100 Å for Sc $2p$ and Sc $3p$ resonant photoemission. The sample thickness was controlled by a quartz-crystal monitor. It seems that the charging up effect is large for Sc2p region, but small for Sc $3p$ region. Measurements were carried out at room temperature.

Photoemission experiments in the Sc $2p$ and F $1s$ reso-

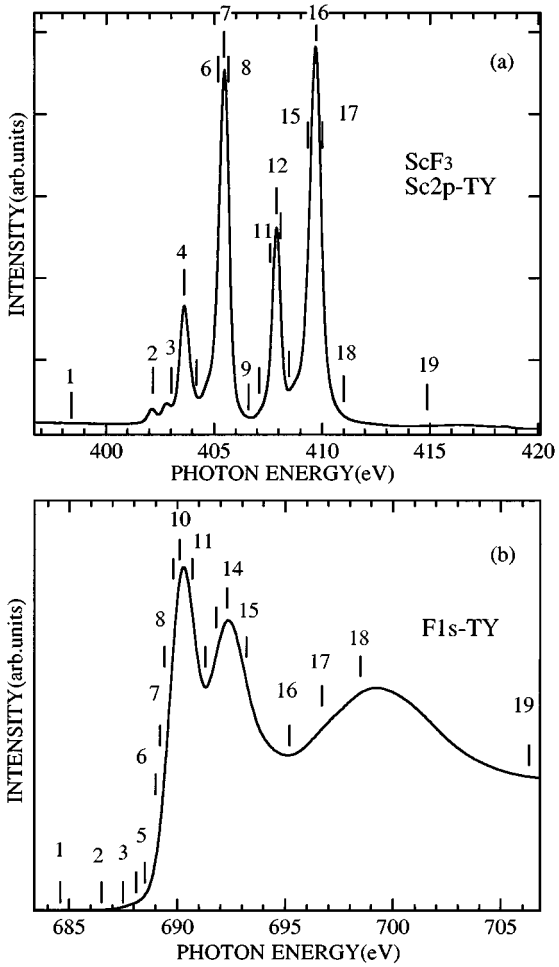

FIG. 1. Total yield (TY) spectra of ScF_3 corresponding to the Sc $2p$ and F $1s$ absorption spectra. The numbers indicate the photon energies, where the resonant-photoemission spectra were measured.

nant photoemission were performed at the beam line BL-2B of Photon Factory at KEK. The base pressure of the sample chamber is below 5×10^{-10} torr. The Vodar-type monochromator was used. The resolution of the monochromator was below 0.5 eV, with a slit width of 50 μm for Sc $2p$ and F $1s$ absorption spectra. A double-stage-type cylindrical mirror analyzer (DCMA) was used for analyzing the kinetic energies of photoelectron. The overall resolution of the photoelectron spectroscopy was about 1 eV for the Sc $2p$ and F $1s$ resonant photoemission spectra. The binding energy of the spectra was calibrated by the photoemission spectra of the evaporated gold, which was used as a substrate.

Experiments in the Sc $3p$ region were carried out at the BL-2 of SOR-RING, a 0.5-GeV electron storage ring of the Institute for Solid State Physics, University of Tokyo. The base pressure of the sample chamber was below 5×10^{-11} torr. A DCMA was used. The overall resolution is about 0.25 eV at the excitation photon energy ($h\nu$) of 40 eV.

III. RESULTS AND DISCUSSIONS

A. Satellite structures

Figure 1(a) shows total yield (TY) spectrum of ScF_3, corresponding to the absorption spectrum from Sc $2p$ core to Sc $3d$ conduction bands. The vertical bars, which are numbered

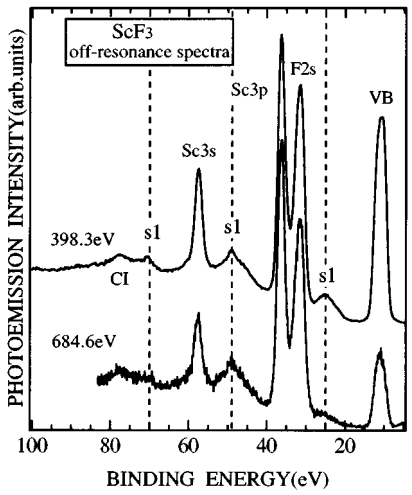

FIG. 2. Photoemission spectra of ScF_3 measured at the energies just below the Sc $2p$ and F $1s$ thresholds, numbered by 1 in Figs. 1(a) and 1(b). The dashed lines denote the $s1$-satellite structures.

from 1 to 19, indicate the selected photon energies for the resonant-photoemission measurements. The spectrum consists of four sharp structures with several pre-edge structures. The linewidth of the main peak is about 0.5 eV. The splitting energy between 4 and 12 (or between 7 and 16) corresponds to a spin-orbit splitting energy of Sc $2p$ core hole. The crystal structure of ScF_3 is WO_3 type, so that a Sc ion is surrounded octahedrally by six F^- ions. Thus, the bands 4 and 7 (or 12 and 16) are the t_{2g} and e_g bands, which are split by the crystal field. It is curious that the intensity of the t_{2g} band is less than that of the e_g band by about $\frac{1}{2}-\frac{1}{3}$, though the number of the empty states is larger by $\frac{3}{2}$. This fact suggests the large $2p$-$3d$ interactions in ScF_3 suppress the absorption intensity to the t_{2g} state. The Sc $2p$ absorption of Sc_2O_3 was carried out by Elango *et al.*[21] and its line shape is similar to that of ScF_3, though its pre-edge structure is much weaker than that of ScF_3.

Figure 1(b) shows TY spectrum, which corresponds to the absorption spectrum from F $1s$ core to F $2p$ components in the conduction bands, which is hybridized with Sc $3d$ components. The vertical bars, which are numbered from 1 to 19, indicate the selected photon energies for the resonant-photoemission measurements. The peaks of 10 and 14 correspond to the crystal-field splitting of t_{2g} and e_g bands. In the case of F $1s$ absorption, the intensity ratio of the t_{2g} and e_g bands is consistent with the empty number of two bands. The broad structure 18 is the higher conduction bands above Sc $3d$ bands, such as Sc $4s$,$4p$ or F $3s$,$3p$ bands.

Figure 2 shows the photoemission spectra measured at $h\nu$=398.3 and 684.6 eV, which correspond to the vertical bars named No. 1 in Figs. 1(a) and 1(b). These spectra are measured at the photon energies below the Sc $2p$ and F $1s$ thresholds, so that Auger spectra are not found in both spectra. In both spectra, valence bands are found around the binding energy (E_B) of about 12 eV. There are two structures in the VB, which are clearly found in the Sc $2p$- and Sc $3p$-resonance spectra in Figs. 3 and 4, as discussed later. Because there are no absorption and reflectance spectra of ScF_3, the band gap of this material has not been known. Since the top of VB is located around E_B=7–8 eV, the large band gap is found to be more than 7–8 eV. Several sharp

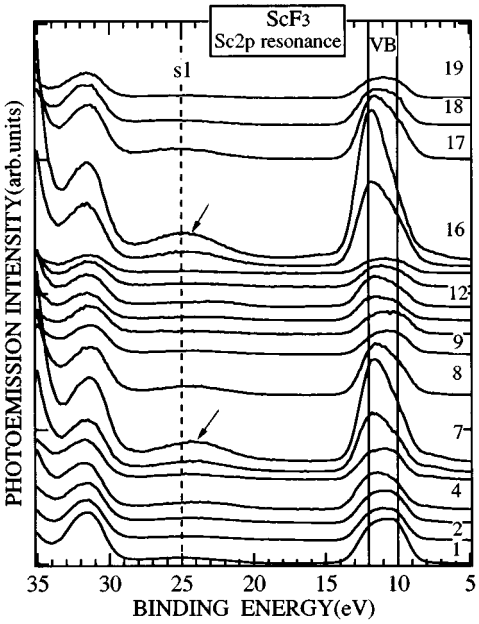

FIG. 3. The Sc $2p$ resonant-photoemission spectra of the VB, which were measured by various photon energies numbered in Fig. 1(a). Arrows indicate the energy shift of the satellite structure by the resonant photoemission.

peaks are found at the binding energy of about 32, 36, and 58 eV in Fig. 2. These peaks correspond to F $2s$-, Sc $3p$-, and Sc $3s$-core lines. Furthermore, one can find the strong $s1$ satellite structures below VB, Sc $3p$, and Sc $3s$ main lines, which are indicated by the dashed lines. All splitting energies from the main lines are almost 13 eV. A very broad satellite (CI) is found beside the $s1$ satellite of Sc $3s$ core. This is a so-called configuration-interaction satellite, due to the $3s^2 3p^4 3d$ configurations.[22]

Figure 5 shows the relation between the main lines and the $s1$ satellite structures, where each main line is set to be located at 0 relative binding energy, with the same peak intensity. The Sc $2p$ photoemission was measured at $h\nu = 715.5$ eV and the others were measured at $h\nu = 398.3$ eV. The satellite structure of Sc $2p$ was already reported by de Boer, Haas, and Sawatzky.[14] The spectrum in Fig. 5 is similar to their spectrum. It is found that the intensity ratios of the satellite structure are very large. Figure 5 shows the energy separations between the main peak and the $s1$ satellite structures are almost 12–13 eV, so that it is suggested that their origins are the same. In general, inelastic-energy-loss spectra have been found below the main peaks.[23] But they mainly consist of the satellite structures, though such inelastic-energy-loss spectra may be overlapped, because their intensity ratios and their line shapes are very different and their energy separations are not exactly the same. The line shape of the VB and $3p$ satellite structures is broad and asymmetric toward the lower binding-energy side. The asymmetry in $3p$ satellite is extremely large. In the next section, the existence of another satellite structure $s2$ will be found to be overlapped at the low energy side of $s1$, by the resonant-photoemission spectra.

B. Sc $2p$-resonant photoemission

Figure 6(a) shows the Sc $2p$ resonant-photoemission spectra of ScF_3 in the $3s$ and $3p$ energy region for $L_3(2p_{3/2})$

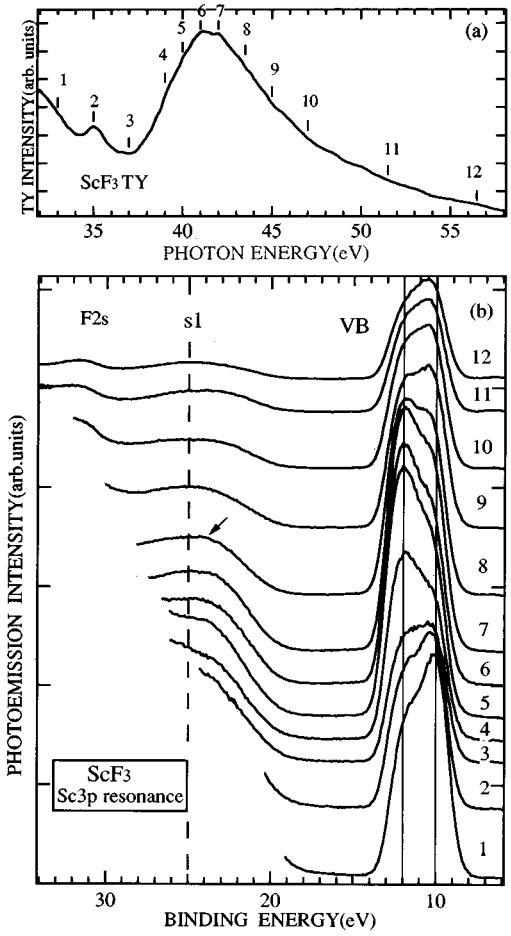

FIG. 4. (a) The total yield (TY) spectrum of ScF_3 and (b) the Sc $3p$ resonant-photoemission spectra measured by various photon energies. The arrow indicates the energy shift of the satellite structure by the resonant photoemission. The numbers indicate the photon energies, where the resonant-photoemission spectra were measured.

absorption edge. The vertical bars around 70–80 eV show the strong $L_{23}M_{23}M_{23}$ Auger. However, Auger components in the other energy region, which involve $3d$ VB electrons, are very weak. Compared with the photoemission spectra of the other transition-metal compounds, the photoemission of ScF_3 has a characteristic feature of weak Auger bands. This fact is related with few $3d$-electron numbers in ScF_3, since the Auger intensity is proportional to the square of $3d$-electron number.

It is clear that the Sc $3s$ and Sc $3p$ main structures are strongly enhanced by the Sc $2p$ resonant photoemission, as shown in Fig. 6. On the other hand, enhancement of the $s1$ satellite of Sc $3p$ line is weak. Though the $s1$ satellite of Sc $3s$ line is overlapped with the strong $L_{23}M_{23}M_{23}$ Auger, its strength seems to be weak when we estimate the photoemission spectra subtracted by the $L_{23}M_{23}M_{23}$ Auger band, which was already measured.[17] It is evident that another satellite, $s2$, is found in the lower-energy side of the $s1$ satellite structure for both Sc $3s$ and Sc $3p$ lines. The $s2$ satellite intensity increases drastically by the resonant enhancement. The splitting energies of $s2$ satellite from the Sc $3p$ and Sc $3s$ main lines are about 9–10 eV. The resonant photoemission is also performed for the $L_2(2p_{1/2})$ absorption edge, as shown in Fig. 6(b). The results are consistent with those in

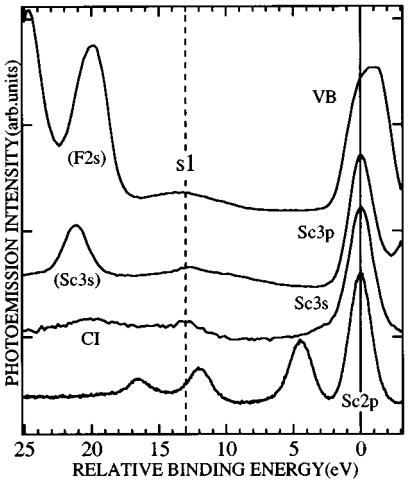

FIG. 5. Photoemission spectra of ScF_3 for various core lines and VB. The dashed line shows the $s1$-satellite structure and the solid line indicates the various main lines.

Fig. 6(a). The Sc $2p$ resonant photoemission[21] was carried out for Sc_2O_3 and the spectra seem to be consistent with those in Figs. 6 though the satellite structure seems to be weak compared with that of ScF_3.

Figure 3 shows the Sc $2p$ resonant photoemission in the VB energy region. From this experiment, it is clear that there are two structures in VB and the enhancement is large for the structure at higher binding energies. The satellite is also enhanced at the $L_3(2p_{3/2})$ absorption edge (Nos. 1–9) and $L_2(2p_{1/2})$ absorption edge (Nos. 10–19). The way of the enhancements for two L_3 and L_2 absorption edges is very similar. At off-resonant excitation, the satellite is located at around 25 eV, but at on resonant excitation, the satellite shifts to lower energies around 24 eV. Arrows indicate the energy shift of the satellite structure by the resonant photoemission.

In this experiment, two different type satellite structures are found in the Sc $3s$ and Sc $3p$ region. One is located around 13 eV below the main peak and is found clearly at off-resonant excitation. This is not enhanced much by the Sc $2p$ resonant photoemission. The other is found around 9–10 eV below the main peak. This is quite weak at off-resonant excitation, but strongly enhanced by the Sc $2p$ resonant photoemission. In the case of VB region, $s2$ satellite is not observed separately from $s1$ satellite. But it shifts to lower energies by about 1 eV at on resonant photoemission. This fact suggests that the $s2$ satellite is located at the low-energy side of the $s1$ satellite even for VB, as in the case of the resonant photoemission of Sc $3s$ and Sc $3p$ satellite bands. However, the enhancement of VB satellite is not so large compared with those of the Sc $3s$- and Sc $3p$-$s2$ satellites.

Here, the problem is the origin of two satellite structures. Obviously, resonant photoemission suggests that both origins are different. The resonant-photoemission process has been known to be the interference effect, which involves $3d$ electrons.[24] Scandium fluoride has no $3d$ electrons nominally. Therefore, $3d$ component is mixed in the material, due to the hybridization effect and resonance is caused only for this $3d$ component. By the CI representation, the hybridization effect of the initial state $|i\rangle$ is represented as follows:

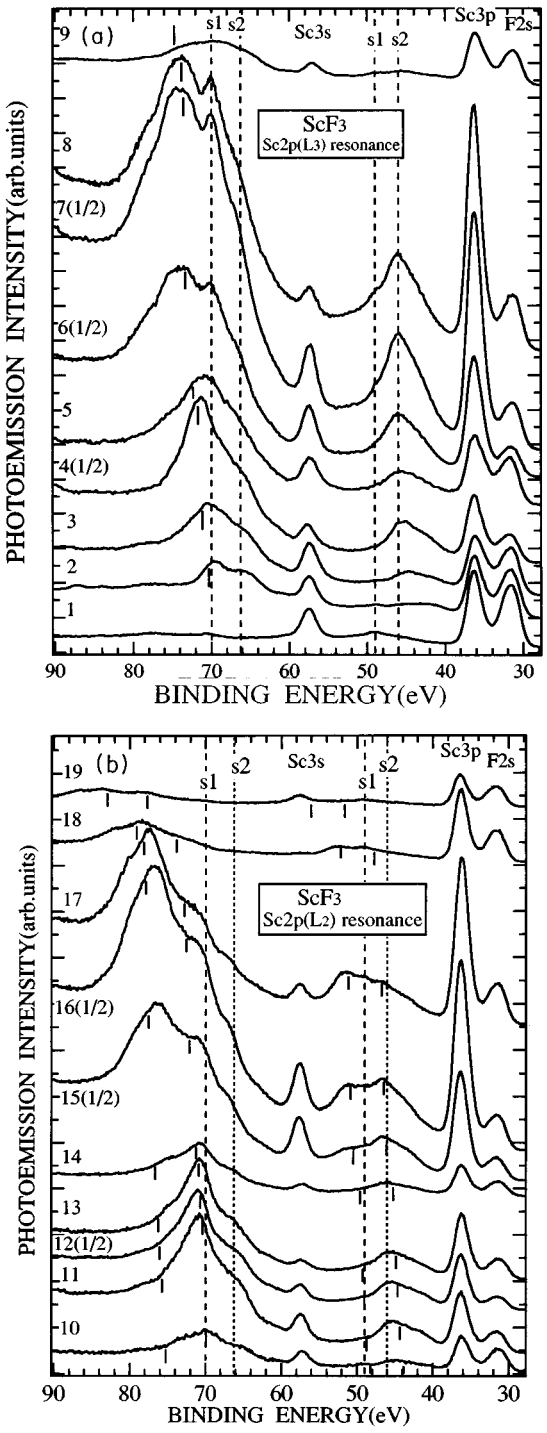

FIG. 6. (a) The resonant-photoemission spectra of the Sc $3p$ and Sc $3s$ lines, which were measured by various photon energies numbered in Fig. 1(a) in the Sc $2p_{3/2}(L_3)$ energy region. (b) The resonant photoemission in the Sc $2p_{1/2}(L_2)$ energy region. The parenthesis beside the photon-energy number is the factor of the intensity. The dashed lines are the $s1$- and $s2$-satellite structures. The vertical bars are the expected Auger lines.

$$|i\rangle = a|3d^0\rangle + b|3d^1\underline{L}\rangle.$$

In the same way, the final state, due to the photoemission process, is expressed by the linear combinations of $3d^0\underline{L}$ and $3d^1\underline{L}^2$ states for the VB and the satellite structures. In a simple mind, the $3d^0\underline{L}$ state is the VB's final state and $3d^1\underline{L}^2$

state is the satellite's final state, because two states are mixed weakly. Although the hybridization energy $V_{\rm eff}$ is large, the Δ is extremely large in ScF_3. Thus, the large hybridization effect is mainly reflected in the large splitting energy ($\approx 2V_{\rm eff}$) between two states, rather than the mixing of two states.

The process of direct photoemission in VB is from the initial state to the final state. On the other hand, the resonant process, which has the interference with the direct photoemission of the main VB, is represented as follows:

$$3d^0 \rightarrow \underline{2p}3d^1 \rightarrow 3d^0\underline{L}, \tag{1}$$

$$3d^1\underline{L} \rightarrow \underline{2p}3d^2\underline{L} \rightarrow 3d^0\underline{L}. \tag{2}$$

The satellite enhancement is caused as follows:

$$3d^0 \rightarrow \underline{2p}3d^1 \rightarrow 3d^1\underline{L}^2, \tag{3}$$

$$3d^1\underline{L} \rightarrow \underline{2p}3d^2\underline{L} \rightarrow 3d^1\underline{L}^2. \tag{4}$$

Among these processes, Eq. (2) involves the intra-atomic Auger decay process, so that the strong enhancement is observed. The others involve the interatomic process, so that the enhancements are weak. Since Eq. (2) gives the resonant photoemission of the higher binding-energy band of VB,[7] this model is consistent with the experimental results.

For the main and satellite $3s$- and $3p$-core photoemission lines, the resonant process is represented as follows:

$$3d^0 \rightarrow \underline{2p}3d^1 \rightarrow \underline{c}3d^0, \tag{5}$$

$$3d^1\underline{L} \rightarrow \underline{2p}3d^2\underline{L} \rightarrow \underline{c}3d^1\underline{L}. \tag{6}$$

Here, $\underline{c}$ denotes the $3s$- or $3p$-core holes. In the case of Sc $3p$ and Sc $3s$ photoemission, both the main and satellite structures should be enhanced by the resonance effect, because they are intra-atomic processes. Thus, it is found that this simple model well explains the strong enhancement of the main and satellite bands.

It is interesting that the way of the resonant enhancement is very different between $s1$ and $s2$ satellites. This fact suggests that the origin of the CT mechanism is different. Very recently, Kotani and co-workers[25,26] calculated the VB and core photoemission of nominally $3d^0$ electron system of early transition-metal compounds. One of the characteristic features in the early transition-metal compounds is that the hybridization strength V between the transition-metal $3d$ and ligand states is very large, in addition to the d-d Coulomb interactions U and CT energy Δ. It has been believed that early transition-metal compounds are the simple Mott-Hubbard materials in the well-known Zaanen, Sawatzky, and Allen scheme.[27] However, recent theoretical analyses show that these materials may belong to another category, because the band gap is not determined only by U or Δ, but mainly by its large hybridization energy V.

When the $3d^0$ system has a strong hybridization effect, $3d^0\underline{L}$ and $3d^1\underline{L}^2$ states split into bonding and antibonding states. These states are combined *in phase* by $3d^0\underline{L}$ and $3d^1\underline{L}^2$, as discussed already. Since $3d^1\underline{L}^2$ has a multiplet structure, because of the existence of $3d$ electron, the orthogonal state to the bonding and antibonding states becomes another nonbonding state. These states are *not in-phase* states, which is located between the bonding and antibonding states.[28,29] Thus, photoemission lines split into three types. By this schematic energy diagram, as shown in Fig. 7, the energy position of $s1$ corresponds to the antibonding state and the $s2$ satellite corresponds to the nonbonding states.

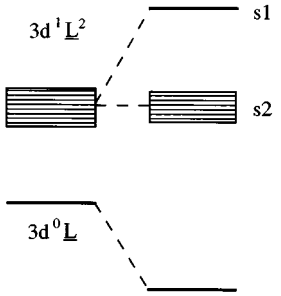

FIG. 7. Schematic diagram of the VB photoemission states of ScF_3 for $s1$- and $s2$-satellite structures.

Since the initial state is an *in-phase* state, the dipole transition is allowed for the main band and $s1$ satellite, but is not allowed for the $s2$ satellite. Thus, only the $s2$ state is very weak in off-resonant photoemission. However, since the on-resonant photoemission is the two-photon process, which does not belong to the dipole transition, the transition to the nonbonding states becomes allowed. Thus, the nonbonding state $s2$ appears in the resonant photoemission. Though these nonbonding-type satellites should exist even in the every transition-metal compound, they still have not been found. It may be because the hybridization effect of the other transition-metal compound is weak compared with the early transition-metal compounds and their complicated structures due to $3d$ electrons smear out their resonance effect.

Very recently Jo and Tanaka[28,29] calculated the Ti $2p$ resonant photoemission of Ti $3p$ and VB region. They suggested that there are two type satellites, in fact. One corresponds to the $s1$-type satellite. Another corresponds to the $s2$-type satellite, which is weak in off-resonant photoemission, but becomes strongly enhanced at the on-resonance excitation. Furthermore, they found that the energy position of the resonant-$s2$-satellite structure shifts to the higher binding energy by about several eV. This energy shift corresponds to the distribution of the t_{2g} and e_g components in the nonbonding multiplet structures, which resonate at t_{2g} and e_g absorption bands, respectively. In fact, such a slight energy shift seems to be found in the $s2$ satellite of Sc $3p$ in this experiment.

C. F 1*s* resonant photoemission

Figure 8 shows the F $1s$ resonant spectra of ScF_3 in the Sc $3p$ and Sc $3s$ binding-energy region, which were measured at the photon energies numbered from 1 to 12 in Fig. 1(b). In the case of F $1s$ resonance, very strong $KVV(KL_{2,3}L_{2,3})$ Auger is observed around E_B=30–35 eV, because VB mainly consists of F $2p$ components. The weak KL_1V and KL_1L_1 Auger lines, which are indicated by vertical bars, are found around 55–60 eV and 75–80 eV. The enhancement at the Sc $3p$ and Sc $3s$ main lines are weak by the F $1s$ resonance excitation. However, it is striking that the resonance effect of the satellite structure is found even at around the F

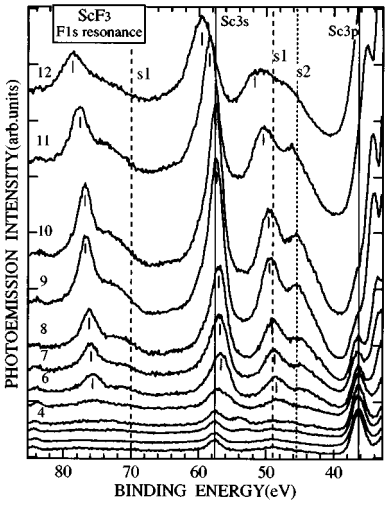

FIG. 8. The F 1s resonant-photoemission spectra of ScF_3 in the Sc 3s and Sc 3p energy region, which were measured by various photon energies numbered in Fig. 1(b). The dashed lines show the $s1$- and $s2$-satellite structures. Vertical bars show the Auger lines.

1s threshold excitation energy. Furthermore, in contrast to Sc 2p resonant photoemission, the $s1$ satellite as well as $s2$ satellite are resonantly enhanced. To our knowledge, resonant enhancement for the ligand core of the transition-metal compound has not been performed. Though the detailed reason for the enhancement mechanism is not known, the existence of both satellites is undoubtedly confirmed by this enhancement. Since the intensity ratios of both satellites to the main peaks increase, they are confirmed again not to be the inelastic energy-loss spectra of the main line.

In a similar way, the F1s resonant enhancement in the VB region is found, as shown in Fig. 9. At off-resonant excitation, the satellite is located at around 25 eV and at on-resonance the satellite is located at around 23 eV. This energy shift is similar to the energy shift of the satellite by the Sc 2p resonant enhancement. So this energy shift may suggest the existence of $s2$ in the VB, as well as Sc 2p resonant photoemission. However, the enhancement in the VB region is weak.

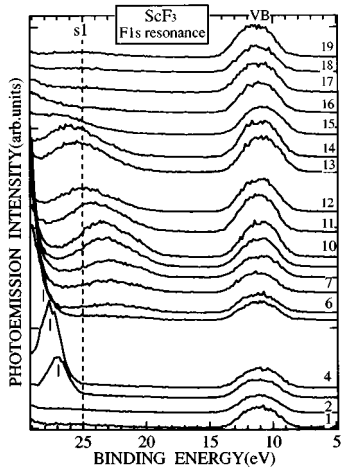

FIG. 9. The F 1s resonant-photoemission spectrum in the VB energy region. Vertical bars show the Auger lines.

It is curious that the resonant photoemission is caused even at F 1s edge. When F 1s core absorption is caused by the synchrotron radiation, the F 1s electron excited to the F 2p state, because of its dipole selection rule. The other component, such as F 3p, is located at much higher conduction band. That is, it is the transition to the ligand hole of the $3d^1\underline{L}$ state, when we use the CI representation. Obviously, in the case of $3d^0$ initial state, such a transition is not able to take place, because there is not a ligand hole. Thus, the resonant processes of Sc 3p and Sc 3s main and satellite lines are represented as follows:

$$3d^1\underline{L} \rightarrow \underline{1s}3d^1 \rightarrow \underline{c}3d^0, \tag{7}$$

$$3d^1\underline{L} \rightarrow \underline{1s}3d^1 \rightarrow \underline{c}3d^1\underline{L}. \tag{8}$$

Both processes involve the interatomic Auger decay processes, so the interference does not become so strong. This is consistent with the experimental results that the resonance effect is not so strong. We believe that the difference of the resonance behavior between F 1s and Sc 2p excitation signifies the difference of the selection rule between them. However, the detailed theoretical studies will be needed.

D. Sc 3p resonant photoemission

In the case of 3p excitation, similar resonant enhancements for the satellite and main structure of VB are also found, as shown by Fig. 4(b). Figure 4(a) shows the TY spectrum, where the numbers show the photon energies, where the resonant-photoemission spectra were measured. It is clear that there are two structures in VB and the structure in higher binding-energy is enhanced. Though the secondary electrons rapidly increase, because of the low excitation energy, the enhancement of the satellite structure is clearly found. Thus, the Sc 3p resonant photoemission spectra are consistent with those of Sc 2p resonant photoemission.

Since the spin-orbit interaction of Sc 3p core hole is small compared with Sc 2p core-hole and 3p-3d interactions are large, a broad structure with a pre-edge structure is found in the TY spectrum and it has a different line shape from that of Sc 2p. The spectrum is very similar to Ti 3p absorption spectrum of TiF_3.[30] However, it is different from those of Ca and K compounds,[31] irrespective of their nominally $3d^0$ configuration. The line shape of Ca and K compounds are very sharp, where several structures due to the spin-orbit interactions and the crystal-field splitting are found. This fact shows that the ScF_3 is a kind of transition metal compound, rather than the alkali-metal or alkali-earth-metal compound. It is clear that the pre-edge structure in 3p TY spectrum is a kind of multiplet structure formed by the strong 3p-3d interactions, which involve the $3d^1\underline{L}$ states. The width of the main peak in ScF_3 strongly depends on the short lifetime of the super-Koster-Kronig decay process, which involves the $3d^1\underline{L}$ components. Thus, the line shape of 3p TY spectra also shows the existence of the $3d^1\underline{L}$ state in ScF_3.

IV. CONCLUSION

Resonant photoemission of ScF_3 was carried out for Sc $2p$ and F $1s$ excitation energy regions. Two kinds of charge-transfer satellites are found with the large energy separations. One is ordinary a charge-transfer-type satellite corresponding to the antibonding state between the $3d^0$ and $3d^1\underline{L}$ states. Another is found to be the nonbonding state. It is found that the latter satellite has a strong resonance at the Sc $2p$ threshold, while both satellites cause the resonance enhancements at the F $1s$ absorption edge. The detailed mechanism of F $1s$ resonance effect has not been known still now.

ACKNOWLEDGMENTS

We greatly acknowledge the useful discussions with Professor T. Ishii. The authors appreciate stimulating discussions with Professor A. Kotani and Professor T. Jo. We would like to thank Professor S. Suga and the staff of his laboratory for their excellent support.

*Author to whom correspondence should be addressed.

[1] T. Uozumi, K. Okada, and A. Kotani, J. Phys. Soc. Jpn. **62**, 2595 (1993).
[2] K. Okada and A. Kotani, J. Electron. Spectrosc. Relat. Phenom. **62**, 131 (1993).
[3] J. C. Parlebas, J. Phys. **2**, 1369 (1992).
[4] J. C. Parelebas, Phys. Status Solidi **178**, 9 (1993).
[5] Zhaoming Zhang, Shin-Puu Jeng, and Victor E. Henrich, Phys. Rev. B **43**, 12 004 (1991).
[6] Kevin E. Smith and Victor E. Henrich, Phys. Rev. B **38**, 9571 (1988).
[7] S. Shin, Y. Tezuka, T. Ishii, and Y. Ueda, Solid State Commun. **87**, 1051 (1993).
[8] A. Fujimori and F. Minami, Phys. Rev. B **30**, 957 (1984).
[9] A. Fujimori, M. Saeki, N. Kimizuka, M. Taniguchi, and S. Suga, Phys. Rev. B **34**, 7318 (1986).
[10] A. Fujimori, F. Minami, K. Siratori, M. Taniguchi, S. Ogawa, and S. Suga, Phys. Rev. B **42**, 7580 (1990).
[11] Jaehoon Park, Seungoh Ryu, Moon-sup Han, and S. J. Oh, Phys. Rev. B **37**, 10 867 (1988).
[12] A. E. Bocquet, T. Mizokawa, T. Saitoh, H. Namatame, and A. Fujimori, Phys. Rev. B **46**, 3771 (1991).
[13] K. Okada and A. Kotani, J. Phys. Soc. Jpn. **61**, 4619 (1992).
[14] D. K. G. de Boer, C. Haas, and G. A. Sawatzky, Phys. Rev. B **29**, 4401 (1984).
[15] B. Wallbank, C. E. Johnson, and I. G. Main, J. Phys. C **6**, L493 (1973).
[16] D. C. Frost, C. A. Mcdowell, and B. Wallbank, Chem. Phys. Lett. **40**, 189 (1976).
[17] D. K. G. deBoer, C. Haas, and G. A. Sawatzky, J. Phys. F. **14**, 2769 (1984).
[18] J. Ghijsen, L. H. Tjeng, H. Eskes, G. A. Sawatzky, and R. L. Johnson, Phys. Rev. B **42**, 2268 (1989).
[19] L. H. Tjeng, C. T. Chen, J. Ghijsen, P. Rudolf, and F. Sette, Phys. Rev. Lett. **67**, 501 (1991).
[20] A. Kakizaki, K. Sugeno, T. Ishii, H. Sugawara, I. Nagakura, and S. Shin, Phys. Rev. B **28**, 1026 (1983).
[21] M. Elango, A. Ausmees, A. Kikas, E. Nommiste, R. Ruus, A. Saar, J. F. van Acker, J. N. Anderson, R. Nyholm, and I. Martinson, Phys. Rev. B **47**, 11 736 (1993).
[22] For example, P. S. Bagus, A. J. Freeman, and F. Sasaki, Phys. Rev. Lett. **30**, 850 (1973).
[23] Kevin W. Goodman and Victor E. Henrich, Phys. Rev. B **50**, 10 450 (1994).
[24] For example, L. C. Davis, J. Appl. Phys. **59**, R25 (1986).
[25] K. Okada, T. Uozumi, and A. Kotani, J. Phys. Soc. Jpn. **63**, 3176 (1994).
[26] T. Uozumi, K. Okada, and A. Kotani, J. Phys. Soc. Jpn. **62**, 2595 (1993).
[27] J. Zaanen, G. A. Sawatzky, and J. W. Allen, Phys. Rev. Lett. **55**, 418 (1985).
[28] A. Tanaka and T. Jo, J. Phys. Soc. Jpn. **63**, 2788 (1994).
[29] T. Jo and A. Tanaka, J. Phys. Soc. Jpn. **64**, 676 (1995).
[30] S. Shin, S. Suga, M. Taniguchi, H. Kanzaki, S. Shibuya, and T. Yamaguchi, J. Phys. Soc. Jpn. **51**, 906 (1982).
[31] For example, G. W. Rubloff, Phys. Rev. B **5**, 662 (1972); C. Satoko S. Sugano, J. Phys. Soc. Jpn. **34**, 701 (1973).